nature research

https://doi.org/10.1038/s41566-020-0689-7

Supplementary information

Tunable free-electron X-ray radiation from van der Waals materials

In the format provided by the authors and unedited

Tunable free-electron X-ray radiation from van der Waals materials

Michael Shentcis, Adam K. Budniak, Xihang Shi, Raphael Dahan, Yaniv Kurman, Michael Kalina, Hanan Herzig Sheinfux, Mark Blei, Mark Kamper Svendsen, Yaron Amouyal, Sefaattin Tongay, Kristian Sommer Thygesen, Frank H.L. Koppens, Efrat Lifshitz, F. Javier García de Abajo, Liang Jie Wong and Ido Kaminer

Supplementary Information

Contents

S.1 Bandwidth of the spectral peaks

The objective of this section is to present the derivation of the bandwidth $\Delta\omega$ of the parametric coherent bremsstrahlung (PCB) energy peaks from Eq. 1. Assuming that the uncertainties of the angle θ and φ follow Gaussian distributions, we use error analysis for independent variables

$$(\Delta\omega)^2 = \left(\frac{\partial\omega}{\partial\varphi}\right)^2 (\Delta\varphi)^2 + \left(\frac{\partial\omega}{\partial\theta}\right)^2 (\Delta\theta)^2 + 2\left(\frac{\partial\omega}{\partial\varphi}\right)\left(\frac{\partial\omega}{\partial\theta}\right)\Delta\varphi\Delta\theta, \tag{S1}$$

where $\Delta\varphi$ is the angular aperture of the detector and $\Delta\theta$ is the angular spread of the electron beam. With the assumption that the parameters θ and φ are uncorrelated, we derive

$$\frac{\Delta\omega}{\omega_m} = \sqrt{\frac{\beta^2 \sin^2\varphi}{(1-\beta\cos\varphi)^2}\Delta\varphi^2 + \tan^2\theta\,\Delta\theta^2}. \quad \text{(S2)}$$

Another factor in this equation has to do with the finite number of layers in the material. For N material layers, the intensity of the emitted radiation scales as,

$$I \propto \left|\sum_{n=1}^{N} e^{in\delta}\right| = \frac{\sin^2(N\delta/2)}{\sin^2(\delta/2)}, \quad \text{(S3)}$$

where $\delta = \omega\left(\frac{d}{\cos\theta}\right)\left(\frac{1}{v} - \frac{\cos\varphi}{c}\right)$ is the phase difference between the emission from consecutive material layers. The FWHM of Eq. S3 varies between $\frac{N\delta}{2} \simeq \pm 1.4$. Hence, the width of the peak is derived from the following condition,

$$\frac{1}{2}\Delta\omega\left(\frac{Nd}{\cos\theta}\right)\left(\frac{1}{v} - \frac{\cos\varphi}{c}\right) = 2.8. \quad \text{(S4)}$$

Noting that $Nd = L$ is the interaction length, the last factor in the peak width formula is,

$$\frac{\Delta\omega}{\omega} = \frac{2.8}{\pi}\frac{d}{mL}. \quad \text{(S5)}$$

Finally, we obtain an expression for the width of the energy peaks from PCB radiation mechanism,

$$\frac{\Delta\omega}{\omega_m} = \frac{\Delta E}{E_m} = \sqrt{0.8\frac{d^2}{m^2L^2} + \frac{\beta^2\sin^2(\varphi)}{[1-\beta\cos(\varphi)]^2}\Delta\varphi_{\mathrm{D}}^2 + \tan^2(\theta)\Delta\theta_{\mathrm{e}}^2}. \quad \text{(S6)}$$

We note that this expression does not include the broadening due to the detector resolution, which also needs to be taken into account in practice. In order to approximate the width of the energy peaks, including all the relevant factors, we combine ΔE obtained from Eq. S6 with the energy resolution of the detector FWHM of ΔE_{Res} for an approximated energy width of $\Delta E_{tot} = \sqrt{\Delta E^2 + \Delta E_{Res}^2}$.

S.2 The angular dependence of PCB

The objective of this section is to show that the brightness values of PCB radiation from van der Waals (vdW) materials (referred to as vdW-PCB in the rest of the supplementary file) can be improved by optimizing the observation angle. Considering 60 keV electrons, for instance, a brightness value $\sim 1 \cdot 10^9 \frac{\text{photons}}{\text{s}\cdot\text{mrad}^2\cdot\text{mm}^2\cdot 0.1\%\text{BW}}$ can be obtained with a current of just 1 nA, which compares favorably with the brightness of conventional X-ray tubes even though the latter operates on much higher currents.

The output photon energy follows the dispersion relation as shown in Eq. 1 of the main text. The theoretical simulation tools we have developed for both the coherent bremsstrahlung (CBS) and the parametric X-ray radiation (PXR) mechanisms (described in the Methods section in the manuscript) are used to investigate the angular dependence of the emitted brightness.

The two examples in Fig. S1 consider electron energies of 60 keV and 300 keV passing through 100 nm-thick WSe_2. φ denotes the angle between the electron velocity and the emission direction and the colormaps are in units of $\frac{\text{photons}}{\text{s}\cdot\text{mrad}^2\cdot\text{mm}^2\cdot 0.1\%\text{BW}}$. The results are azimuthally symmetric, as we consider an average over the electron illumination on the crystal. The simulation is performed for electron current of 1 nA and electron spot diameter of 1 nm.

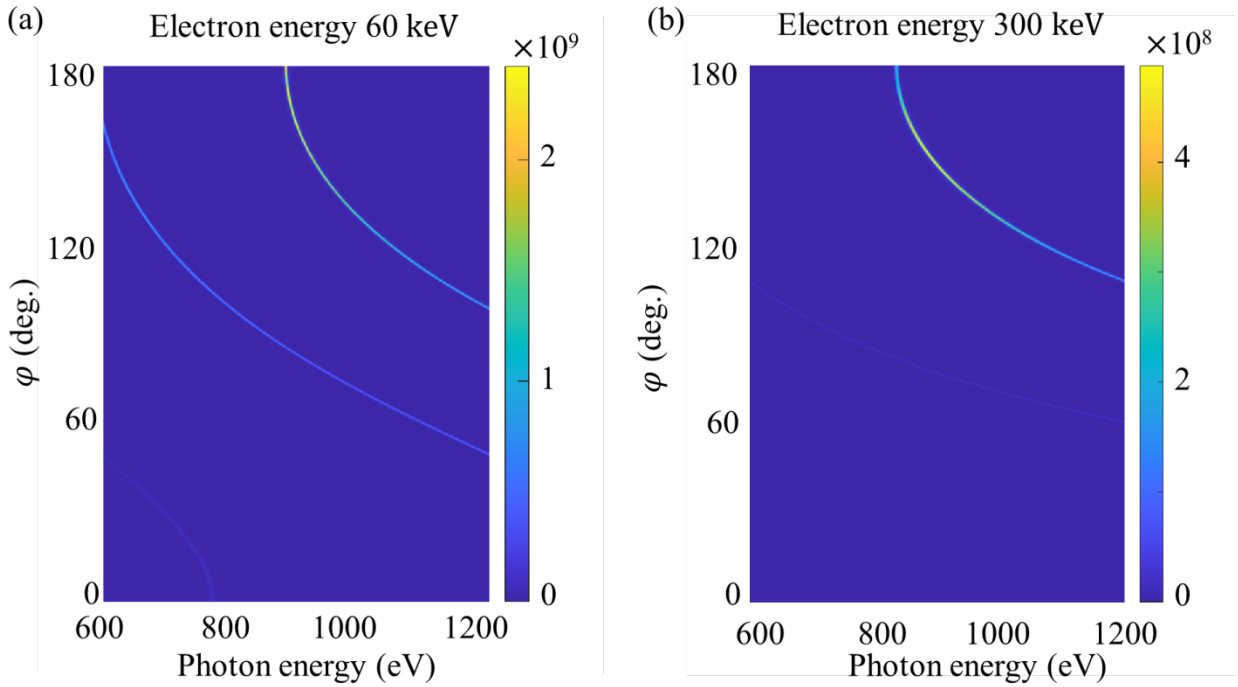

Figure S1: Angular distribution of the brightness of vdW-PCB. The simulation considers radiation emitted from electrons of energy (a) 60 keV and (b) 300 keV passing through WSe_2 of 100 nm thickness. φ is the angle between the electron velocity and the emission direction. The electron current is 1 nA and the electron beam illumination diameter is 1 nm. The unit of the colormaps is $\frac{\text{photons}}{\text{s}\cdot\text{mrad}^2\cdot\text{mm}^2\cdot 0.1\%\text{BW}}$.

S.3 Brightness variation over interaction length

The objective of this section is to show the potential of enhancing the vdW-PCB brightness by increasing the interaction length.

Consider an electron energy of 60 keV, propagating through WSe_2 and emitting radiation at an angle of 121º. Figure S2 presents the energy spectrum under different interaction lengths ranging from 10 nm to 200 nm. We see that the bandwidth of each peak decreases with increased interaction length. Figure S3 shows that the brightness is proportional to the interaction length squared. We consider a current of 1 nA and an electron beam diameter of 1 nm in the calculation.

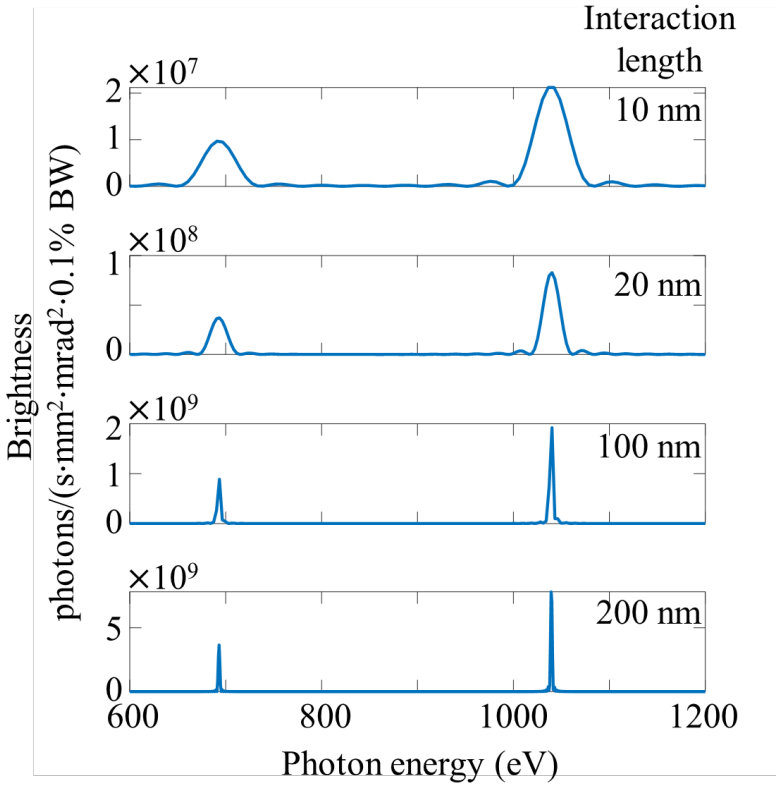

Figure S2: PCB energy spectrum variation with interaction length. The energy spectrum of radiation emitted at 121º from a 60 keV electron beam propagating through WSe_2 sample. Comparing several interaction lengths, ranging from 10 nm to 200 nm. Two energy peaks that correspond to emission orders m=2 and m=3 (Eq. 1), are centered around 693 eV and 1039 eV. The bandwidth decreases while the brightness is enhanced for longer interaction lengths. The electron has 1 nA current and 1 nm spot diameter.

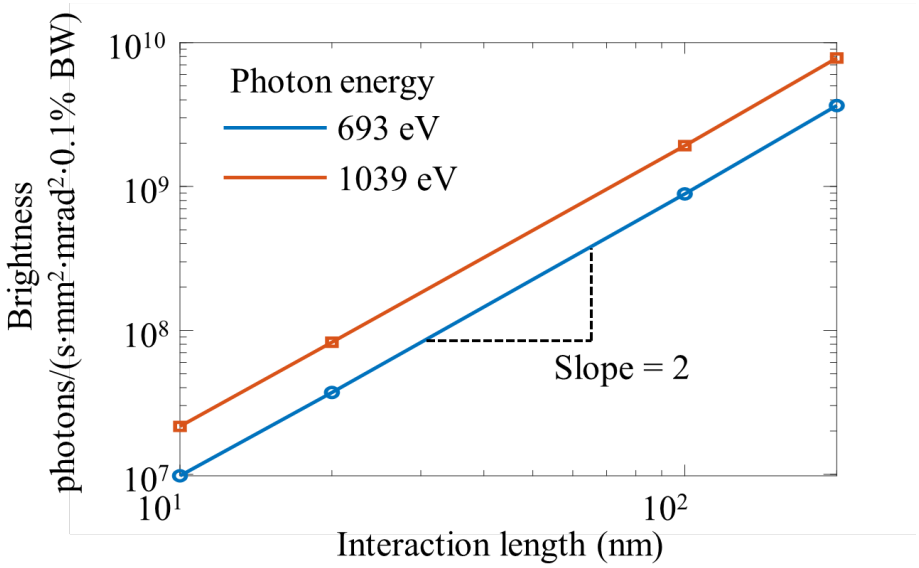

Figure S3: The scaling of PCB brightness as a function of the interaction length. Examining the same energy peaks, and under the same conditions as in Fig. S2. i.e., 693 eV and 1039 eV energy peaks corresponding to emission orders m=2 and m=3 according to Eq. 1 for radiation emitted in angle 121° with respect to the 60 keV propagating electron direction. As previously, 1 nA electron current and 1 nm electron beam spot diameter are considered. The brightness scales as the interaction length squared.

S.4 VdW-PCB from MeV electrons

The objective of this section is to show a prediction of the brightness values predicted for vdW-PCB in the hard X-ray regime. This energy is obtainable by using higher energy electrons (examples shown for electron energies of 1 MeV and 5 MeV) that can be produced from compact sources. In this electron energy regime, we consider the radiation emitted in a small cone along the direction of the incident electrons, as it is the strongest direction of emission. We see that under such conditions, the brightness of radiation emitted from CBS mechanism is favorable over PXR generated radiation, in contrast to the relationship between the mechanisms in the soft X-ray regime.

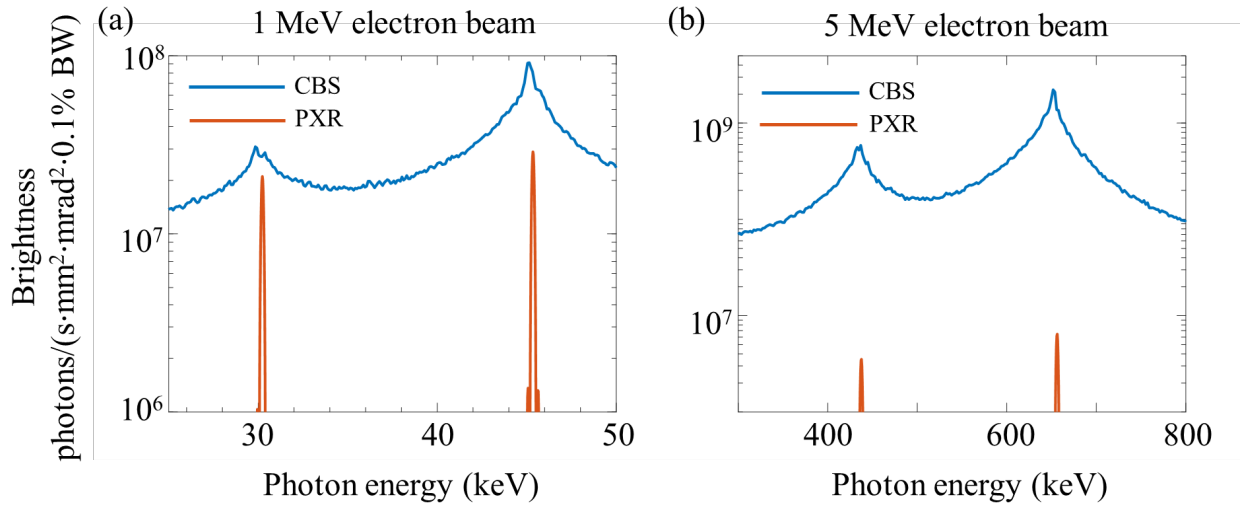

Figure S4: Energy spectrum of on-axis CBS and PXR radiation from 1 MeV and 5 MeV electrons. The radiation is emitted from a 100 nm thick WSe_2 sample in the forward direction, parallel to the direction of the incident electron beam. 1 nA electron current and 1 nm electron beam spot diameter.

S.5 Tradeoffs in increasing vdW-PCB brightness and the role of space charge

The objective of this section is to discuss the limit imposed by space charge on the brightness of vdW-PCB, and to identify the optimal parameters for achieving the maximal brightness.

The brightness of X-ray sources is directly proportional to current and inversely proportional to the electron beam spot size. However, due to space charge, i.e., inter-electron repulsion, the diversion of electron beam is much more significant for strong electron currents and smaller spot sizes. Our simulations show that the radiation energy peaks are significantly deviate (> 5%) from their original values as the electron beam divergence exceeds 0.1 degrees. If we consider a WSe_2 thin-film of thickness 100 nm, the effective interaction length is limited firstly by the physical length of the material (in this case 100 nm), and secondly by the point at which the divergence angle of the electron beam exceeds 0.1 degrees. Therefore, a tradeoff exists between the achievable brightness and the monochromaticity of the emitted radiation. We illustrate this tradeoff using the approach in Eq. S5 in Supplementary Section S.1 and considering that the brightness of X-ray source is proportional to the current, to the interaction length squared, and inversely proportional to the electron beam spot size. Fig. S5 shows the potential increase over brightness compared to the brightness of $\sim 1 \cdot 10^9 \frac{\text{photons}}{\text{s}\cdot\text{mrad}^2\cdot\text{mm}^2\cdot 0.1\%\text{BW}}$, achievable under conventional experimental conditions of transmission electron microscopes (electron current of 1 nA and electron beam spot diameter of 1 nm). We observe the limited saturated brightness by increasing the current while keeping a fixed initial electron beam size. This scenario will cause divergence of the electron beam due to space-charge, which will reduce the interaction length leading to reduction of the brightness. The top achieved brightness can be enhanced by factor of 10^7, leading to a theoretical achievable value of $10^{16} \frac{\text{photons}}{\text{s}\cdot\text{mrad}^2\cdot\text{mm}^2\cdot 0.1\%\text{BW}}$.

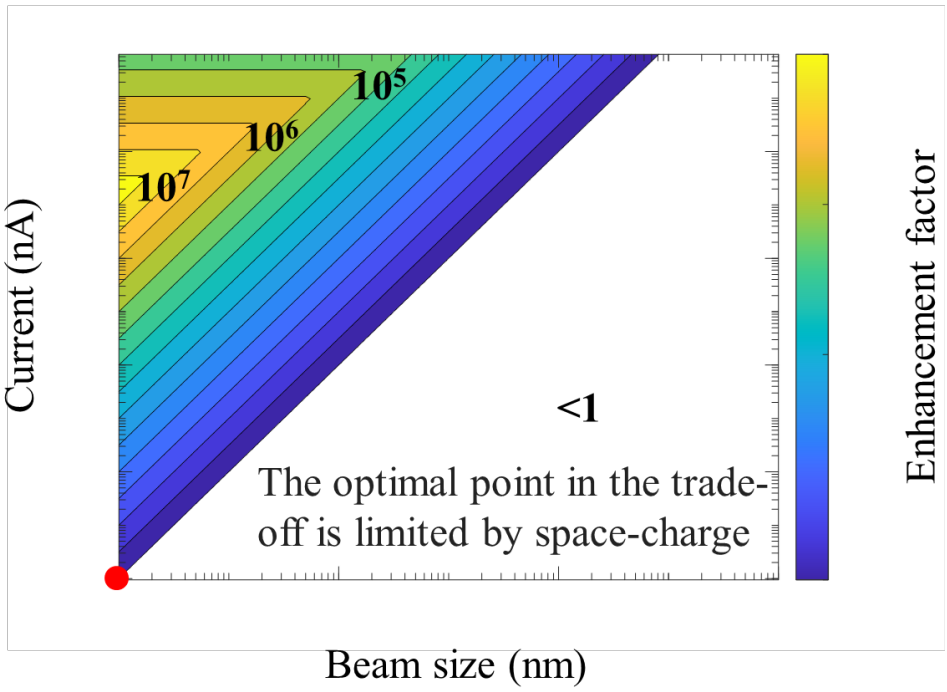

Figure S5: The enhancement factor of brightness (compared to 1 nA current and 1 nm electron beam diameter) with different combinations of beam size and electron current. The other conditions are maintained the same as in the original brightness prediction in the manuscript (i.e. PCB radiation emitted in 121° with respect to the incident electron beam, generated from 60 keV electrons passing through 100 nm thick WSe_2 sample). We can see that beyond a certain current, it is not beneficial to increase the brightness further because space charge effect causes the beam to spread and practically reduces the effective interaction length inside the crystal.

S.6 Calibration of the total photon count

The objective of this section is to present the photon counts by using the simulation results incorporated in Fig. 1 of the main text. Figure 1 shows the spectrum of the emitted radiation from the WSe_2 structure, presenting both experimental and theoretical results using the simulation tools we developed for CBS and PXR. These numerical tools were used to estimate the photon counts, as shown in an example in Fig. S6, considering a 1 nA electron beam with energy of 300 keV, interacting with a 100 nm thick WSe_2 sample.

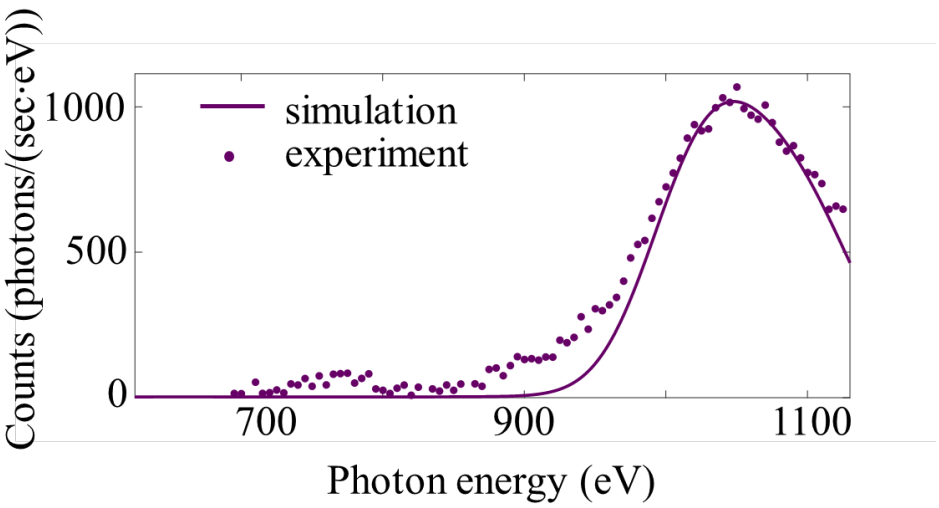

Figure S6: Photon counts of PCB radiation. The radiation spectrum presents PCB radiation from 100 nm WSe_2 structure, emitted in 121° with respect to the incident electron beam. The electron current and energy are 1 nA and 300 keV respectively. The estimation was done by fitting the theoretical prediction to the experimental results, using the simulation tools which are discussed in the Methods section of the main text.

S.7 Diffraction of X-ray radiation created inside the crystal

The objective of this section is to explore the impact of X-ray diffraction of the emitted PCB radiation in the material. The diffraction of X-ray emitted inside the crystal may explain small disagreements between the theoretical prediction and the experimental results. We also note how the vdW-PCB source provides a unique perspective for exploring effects of X-ray diffraction.

In our simulation of both PXR and CBS, the radiation results from direct interference of emission from multiple points within the WSe_2 crystal. The emitted radiation can be further diffracted by the periodic arrangement of atoms in the crystals, following the rules of Bragg scattering. It is to be noted that the X-ray is created and diffracted inside the crystal at the same time. We show the schematic representation of the X-ray diffraction in both real and momentum space in Fig. S7.

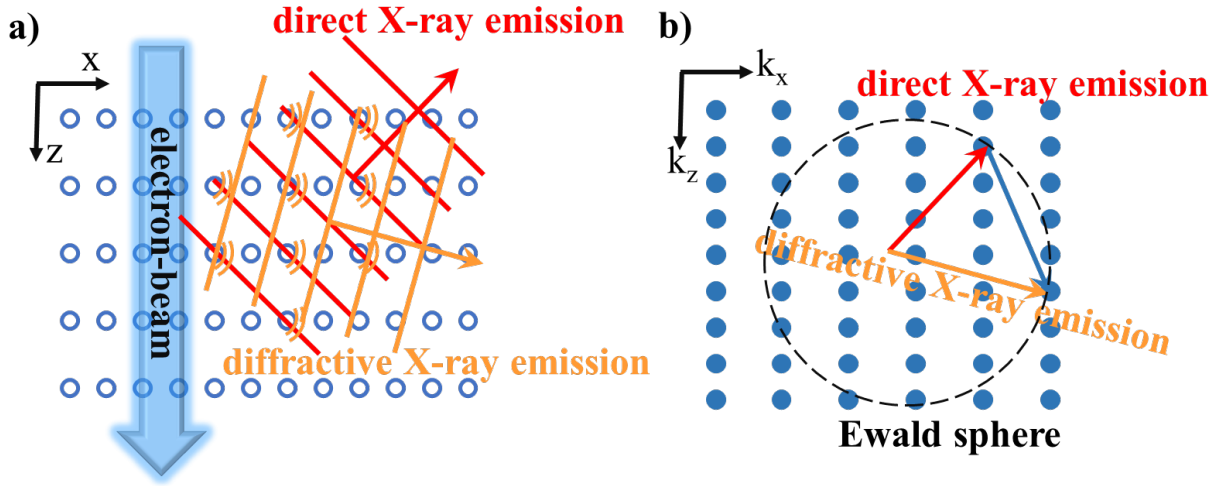

Figure S7: Real (a) and momentum (b) space schematic representation of direct X-ray emission due to PCB (red) and emission associated with diffraction of the latter (orange). (a) The electron beam (blue) produces direct coherent emission emanating from the atoms that are within the range of its associated evanescent electromagnetic field. For a given X-ray emission energy, constructive interference between emitters leads to specific directions of emission (red curves). The directly emitted X-rays are in turn elastically scattered by other atoms in the crystal (conventional X-ray diffraction), leading to additional orders and additional emission directions. (b) In momentum space, the direct emission wave vector (red) can be scattered by diffraction (i.e., addition of a lattice vector in blue) to other points within the sphere of constant X-ray energy (i.e., X-ray energy is conserved during elastic scattering). Along some given emission angles, different spectral features can coexist due to contributions from both direct emission at some energy and diffraction through the above scheme at different energies.

S.8 Coherence of PCB

There are several meanings of the word "coherence" in the context of radiation sources from free electrons, and this section explains the different effects described by this word.

(1) For radiation from multiple electrons to be coherent one needs electrons to be bunched. The radiation from multiple electrons in our experiment is not coherent in this sense. The electrons in the TEM that we used arrive at random times and at currents that make them too spaced-apart to result in coherent radiation in this sense. The use of alternative nano-modulated electrons can generate vdW-PCB radiation that is coherent from multiple electrons.

(2) PCB radiation from each individual electron also has coherence properties as it is emitted from an extended structure (many periods of the lattice) simultaneously. This is where the electron velocity alters the radiation angle, as it correlates between the phases of the emission from different points inside the vdW material. Without this coherent relation between the different emission points, the radiation cannot have the observed spectral peaks at each velocity. Therefore, the monochromaticity we observe is already a measure of this coherence relation. Quantitatively, our data shows that the emission is coherent along an interaction length of ~100 nm inside the crystal, which corresponds to ~150 periods of the vdW material.

(3) One can also consider the transverse coherence of the radiation. The radiation from each different electron can have high transverse coherence because of the small area from which the radiation is emitted. The limit on the transverse coherence is the emitter size – which in our case is under 100 nm (depending on tradeoffs with the current as we discussed above). In comparison, typical X-ray tubes use much wider electron beam spot sizes (~mm), which results in much lower transverse coherence. To measure the transverse coherence, one would need to go through a diffraction experiment with the outgoing X-rays (or do a double-slit experiment, or holography). Such a test would require a specialized proprietary setup that differs than our electron microscope in several geometrical considerations, to allow for additional elements between the sample and the detector.

Altogether, the coherent properties (points 2 and 3) of the vdW-PCB mechanism give it certain advantages in comparison with X-ray tubes, which are incoherent in all of the above meanings of "coherence".

[1] Wong, L. J., Kaminer, I., Ilic, O., Joannopoulos, J. D. and Soljačić, M. Towards graphene plasmon-based free-electron infrared to X-ray sources. *Nature Photon.* **10**, 46 (2016).